

Simultaneous measurements of droplet characteristics and surface thermal behaviour to study spray cooling with pulsed sprays

by

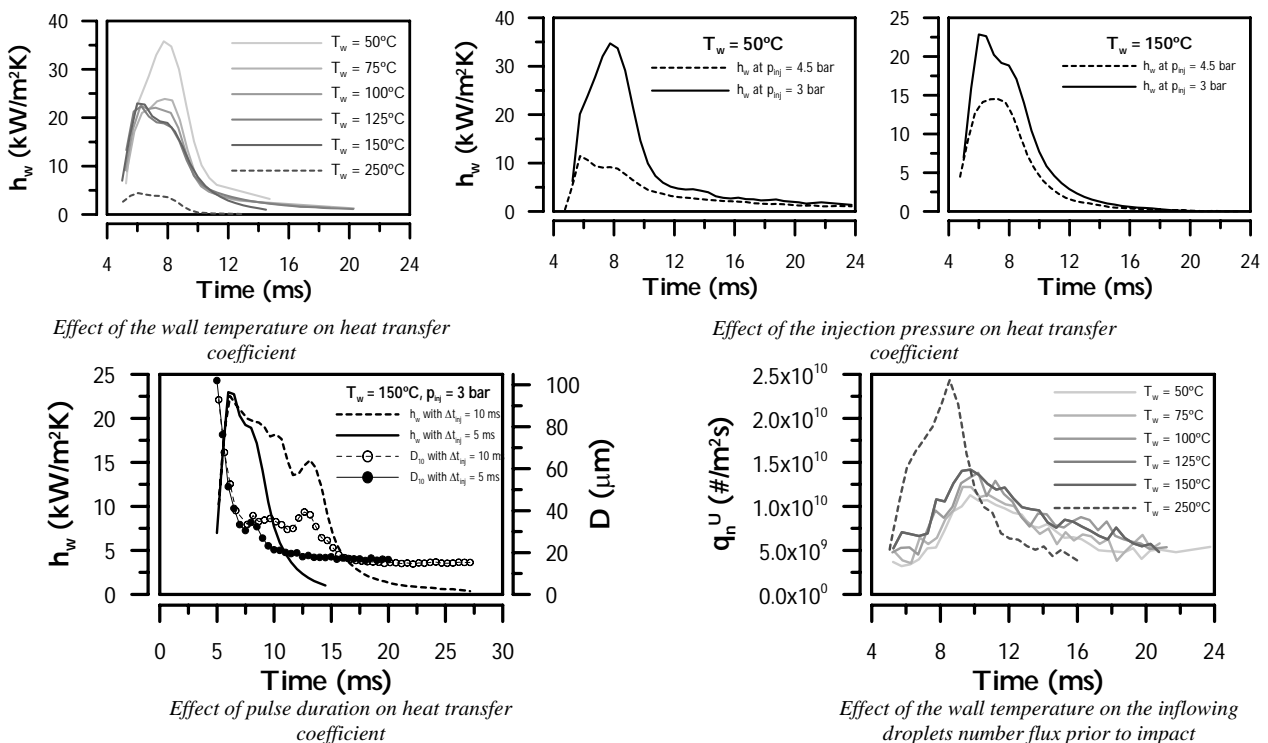
H. M. Loureiro, M.R.O. Panão and A.L.N. Moreira⁽¹⁾

Instituto Superior Técnico
 Mechanical Engineering Department
 Av. Rovisco Pais, 1049 - 001 Lisboa; Portugal
⁽¹⁾E-Mail: moreira@dem.ist.utl.pt

ABSTRACT

The present paper describes an experimental methodology devised to study spray cooling with pulsed sprays combining a two-component Phase Doppler Anemometer with fast response surface thermocouples. The hardware allows simultaneous acquisition of Doppler and thermocouple signals which are processed in Matlab to estimate the time-varying heat flux and fluid-dynamic characteristics of the spray during impact. The time resolution of the acquisition system is limited by the data rate of validation of the Phase Doppler Anemometer, but it has been shown to be accurate for the characterization of spray-cooling processes with spurt durations of the order of 5 ms.

The experimental system is tested in a preliminary study of the effect of surface temperature, injection pressure, duration and frequency on the heat flux removed by an intermittent gasoline spray impinging perpendicular to a heated surface. The experiments show that the heat flux increases as the temperature of the surface increases, but the convection coefficient decreases. For low values of the surface temperature (e. g., 50°C), cooling of the surface is mainly due to heat transfer with the evaporating liquid film formed during injection. It is suggested that dynamic variations of the film induced by interaction with impacting droplets may improve the rate of heat transfer. It is also observed that the heat flux decreases when the pressure of injection is increased from 3 bar to 4,5 bar, but it increases with the duration of injection. Furthermore, it is clear that the time variation of the heat flux during injection is strongly related with the time variation of droplet size distribution. However, PDA measurements were not made close enough to the wall, for an accurate correlation between these and the convective heat transfer coefficient. The analysis also considers the effects of the rising plume induced by surface heating on spray characteristics prior to impact. Although it is observed a decrease of the mean size of droplets prior to impact, major effects occur at the tail of the spray, when small and slow secondary droplets are entrained into the ring vortex induced by shear stresses at the edge of the spray.



1. INTRODUCTION

Spray impingement on hot surfaces has the capability of removing large amounts of energy at low temperatures through the latent heat of evaporation. It is now widely used in several industrial and technological applications in which controlled, rapid and effective cooling performance is required and is considered to be one of the key technologies for developing thermal management systems.

A considerable amount of experimental and theoretical work has been performed to develop heat transfer correlations based on steady state flow bench setups with heated surfaces, which provided valuable insights to the heat exchange between the surface and spray droplets, *e. g.*, Jia and Qiu (2003). It has been shown that heat transfer rates much higher than can be attained using pool boiling are possible with sprays since the vapour removal from the surface is much easier. This leads to think that the thermal interaction between the spray droplets and the vapour during pre-impact have a significant influence on the heat transfer in spray cooling, as suggested by Yoshida et al. (2001). In fact, González and Black (1997) studied the interaction between spray and buoyant jet arising from the heated surface and pointed out a considerable reduction in droplet velocity due to the counter-flowing buoyant vapour jet, although they used a low range of Reynolds values. It is therefore expected that the capabilities of spray cooling for intensive and accurately control heat removal can be enhanced with pulsed sprays by proper matching the duration and frequency of injection. A proper investigation to optimize such procedure requires simultaneous measurements of droplet characteristics and surface thermal behaviour on impacting pulsed sprays.

Moreover, spray impingement against hot surfaces occur in other practical situations, which also require a comprehensive knowledge of the energy flow pathways that determine the surface temperature and the interaction of the liquid spray with the surface. One example deals with the development of fuel injection systems in internal combustion engines: *i*) in a spark ignition engine with port fuel injection, fuel injection often targets the back of the intake valve to promote fuel vaporization, since the intake valve is both the hottest part in the intake system and also it is the fastest to come up to a higher temperature in the engine-warm-up process; however, a significant portion of the fuel injected during engine-warm-up deposits onto the port surfaces and generates a thin film, which does not have sufficient time to vaporize prior to the intake stroke and thus leading to unburned hydrocarbons in the exhaust gas. *ii*) In direct injection engines, fuel impingement onto the piston head may be intentionally used to control the spatial distribution of the spray within the cylinder, or is to be avoided to promote a homogeneous ignitable mixture, depending on the mode of operation. In all cases impingement of the fuel spray onto interposed surfaces affects mixture preparation and, therefore, the performance of the engine.

Most of previous experiments performed on IC engines focused on post-impact behaviours, such as the heat flux between the spray and the target surface, based on surface temperature measurements (*e. g.*, Shayler *at al.*, 1996 and Cowart and Cheng, 1999). Only a few considered the interrelation between heat transfer and droplet characteristics of the impinging spray, which required the use of simplified laboratory configurations where some of the complexities of practical flows were removed, even though considering IC fuel injection systems, *e. g.* Arcoumanis and Chang (1993) and Cutter (1996). However, simultaneous measurements of the flow and heat transfer effects have not been provided yet, which again are still required in order to account for the effects of the transient nature of fuel injection systems.

In this work, a post-process algorithm is devised to synchronize data acquired simultaneously by a temperature acquisition system and a phase Doppler anemometer. The algorithm is implemented in Matlab and applied to an intermittent gasoline spray impacting perpendicular onto a heated surface, with the purpose of performing a parametric analysis on the effects of the wall temperature, injection pressure and pulse duration in the wall heat flux removed by spray cooling. Besides, an attempt is made to evaluate the influence of the wall temperature in the characteristics of the incident spray.

2. INSTRUMENTATION AND DATA PROCESS

2.1 Experimental Arrangement

The experimental setup was designed to study a transient gasoline spray impinging onto a flat plate under cross-flow conditions, as shown in Fig. 1 (Panão and Moreira, 2002a, 2002b). However, the results reported here do not consider the presence of the cross-flow. The spray is generated by a pintle-type injector with a hollow-cone structure and the injection pressure is controlled by a pressure regulation valve. The frequency and duration of injection are controlled by an NI5411 arbitrary function generator. The injector has an electromechanical delay relatively to the electronic pulse sent to open and close the pintle. These delays were determined to be 1.6 and 1.3 ms, respectively, and found to be independent of pressure and injection duration. Therefore, the effective injection period is always 0.3 ms shorter than expected. The fluid injected is gasoline with density of 758 kg/m^3 , dynamic viscosity of $4.66 \times 10^{-4} \text{ kg/m}\cdot\text{s}$, refractive

index of 1.44 and surface tension of 19.4 mN/m. The impinging aluminium plate is located 55 mm below the injector nozzle and is 12 mm thick to avoid that fluctuations from the spray cooling event perturb the temperature at the bottom surface, which is kept constant for heat flux measurement purposes. The plate has a thermal diffusivity of $6.676 \times 10^{-5} \text{ m}^2/\text{s}$ and a thermal conductivity of 164 W/m-K.

The target surface is heated by an electric resistance isolated at the bottom. The temperature of the surface is measured by three NANMAC fast-response eroding-type thermocouples displaced in an L-shape. The junctions of the thermocouples are made by rubbing the surface with an abrasive cloth until the thermocouple resistance is between 8 and 12Ω to insure a response time in the order of $10 \mu\text{s}$. A thermographic analysis showed that the thermocouples do not alter the uniform temperature distribution of the target. The thermocouple signals are amplified with a gain of 300 and digitized at a sample rate of 50 kHz. Electronic noise is quantified to be of the order of $\pm 0.8^\circ\text{C}$ for the range of wall temperatures considered here. The system used to measure the wall temperature is schematically shown in Fig.2.

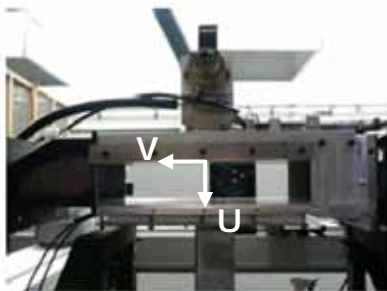


Fig. 1 Flow Configuration (Panão and Moreira, 2002a, 2002b).

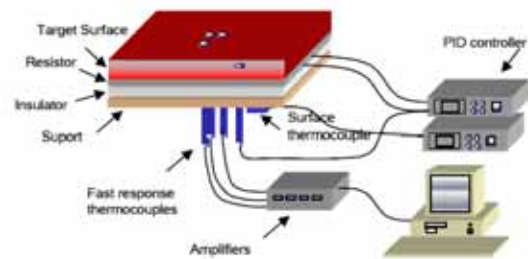


Fig. 2 Temperature data acquisition system.

Local time-resolved measurements of droplet size, velocity and flux are simultaneously measured with a two-component phase Doppler DANTEC system consisting of a 55X transmitting optics, a 57x10 PDA receiving optics. The axial (U) and radial (V) velocity directions are represented in Fig. 1 and more details about the PDA optical configuration are described in table 1. All the PDA measurements reported here were made at the geometrical axis of the injector ($r=0 \text{ mm}$) and 5 mm above the target.

<u>Transmitting Optics</u>	<u>Value</u>
Laser Power	300 mW
Wavelengths	514.5 and 488 nm
Beam spacing	60 mm
Transmitter Focal Length	500 mm
Frequency Shift	40 MHz

<u>Receiving Optics</u>	<u>Value</u>
Scattering Angle	30°
Receiver Focal Length	500 mm
<u>Processor Parameters</u>	<u>Value</u>
U and V signal bandwidth	12 MHz
S/N Validation	0 dB
Spherical Validation	10%

Table 1 – PDA optical configuration

2.2 Measurement Methodology

Electrical voltages from the thermocouples are read into computer memory through a plug-in data acquisition board (DAQ) with eight channels that contains analog-to-digital converters. Data acquisition is controlled by a program developed in Matlab. Doppler signals are acquired and processed for droplet diameter, two velocity components and fluxes by a 58N10 DANTEC Covariance processor. Each measurement system uses a separate computer, but both are triggered by the same electronic pulse used to trigger fuel injection. This signal is further used for timing purposes as the start of injection (SOI). An ideal sampling procedure could be devised, which samples continuously both signals up to achieve sampling sizes large enough for the resulting processed measurements to be statistically independent. However, this is not possible due to two orders of constraints.

The former is that validated Doppler signals are sampled at a much slower rate than temperature signals. An adequate sample size of Doppler signals would, therefore, overflow the DAQ computer board with temperature data. The second order of constraints derives from the fact that the heating system can not keep the surface temperature constant at the start of each injection. A practical sampling procedure must then consider these two issues: 1st) a reasonable sample size of validated Doppler signals and 2nd) a constant surface temperature at SOI. The first issue is accomplished by performing a series of n injections, being the number of series dependent on the required sample size. The second issue is accomplished by stating a maximum deviation between the prescribed initial temperature and the temperature read at SOI by the three surface thermocouples. The measurements reported here consider a maximum deviation of $\varepsilon_w = 1.5\%$. Therefore, the n^{th} injection of each series is achieved when the target temperature at SOI is 1.5% below the temperature at the start of the 1st injection.

Fig. 3 shows the deviation of the target temperature at SOI along several series of 20 injections, for different injection conditions (*e. g.*, duration and pressure) when the initial target temperature is $T_w^{1st} = 150^\circ\text{C}$. The Figure shows that the number n of allowed injections should be around 12-16 for duration of injection of 10 ms and 14-20 for duration of injection of 5 ms.

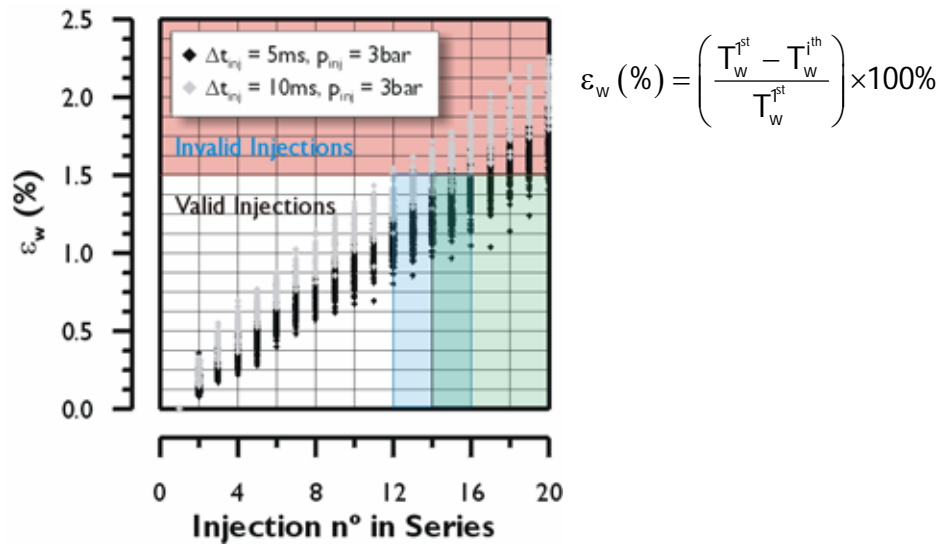


Fig. 3 Wall temperature decay along 20 injections for several injection conditions (*e. g.*, duration and pressure) when the initial target temperature is $T_w^{1st} = 150^\circ\text{C}$

Based on these criteria, the number n of injections in each series is prescribed at 20 injections and the number of series is chosen depending on the validation rate of Doppler signals.

2.3 Data Acquisition and Synchronization Algorithm

Figure 4 depicts the procedure of data acquisition: the TTL signal generated by the function generator to trigger the fuel injector is used as a reset pulse for, both, the temperature and the Doppler acquisition systems. Once the acquisition program is started, the DAQ board continuously monitors the thermocouples signals waiting for a trigger from the function generator to start measuring. After a series of injections, another program downloads the temperature data from the DAQ board, but instead of the complete dataset, it only downloads data acquired between an instant before the reset pulse (BRP) up to an instant right after the start of the injection (ASOI) pulse. These instants were set in our experiment to 5 (BRP) and 50 ms (ASOI), respectively. The 5 ms acquired before the pulse are used to calculate the wall temperature at the beginning of an injection cycle and also to check if the temperature distribution is uniform over the impact surface. While in the temperature acquisition system each injection is recorded in a different data file, for the PDA data a whole series is recorded. A procedure is then followed to generate a file of synchronized data from the individual data sampled, as shown in Figure 5.

At a first step, the reset pulse of the first injection is used as a time frame to synchronize both data file. Then, at a second step, the n reset pulses of the n injections in each series are picked to be used as time frames to perform phase-

average calculations. Finally, after applying a moving average to the temperature profile at step 3, two tasks are performed in order to reduce the effects of electronic noise: task 1) calculate the wall heat flux from the temperature profile according to Reichelt *et al.* (2002); task 2) at each instant a droplet is validated, the wall temperature and the wall heat flux are calculated by interpolation. The second task considers that the temperature is equivalent to a continuous phase in a multiphase flow, as exemplified in Fig. 6.

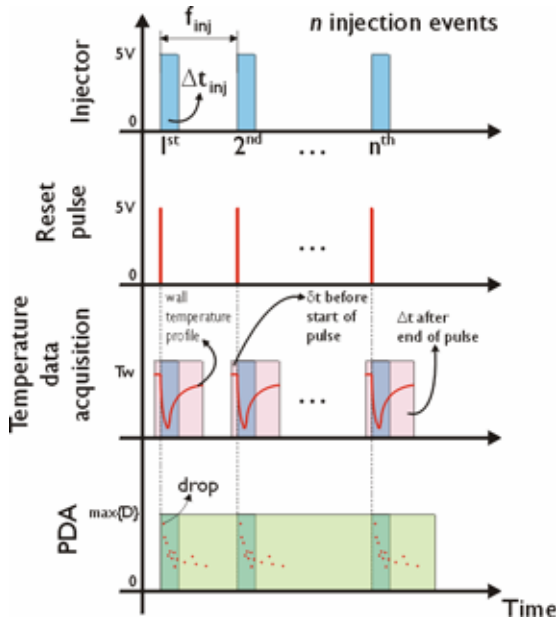


Fig. 4 Temporal diagram for simultaneous measurements of wall temperature, size and velocity of droplets in each series of n injections

The method to determine the heat flux profile assumes a uniform temperature distribution prior to spray impingement, a constant temperature at the bottom surface of the impinging plate and unidirectional conduction perpendicular to the surface. Details about the deduction of the algorithm used to calculate the wall heat flux may be found in Reichelt *et al.* (2002).

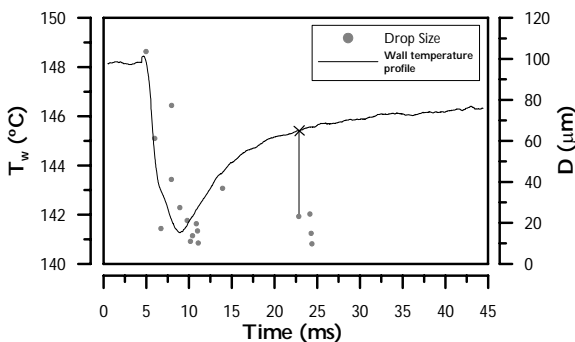


Fig. 6 Temporal evolution of the wall temperature and the associated temperature at the moment a droplet crosses the PDA detection volume for an injection cycle.

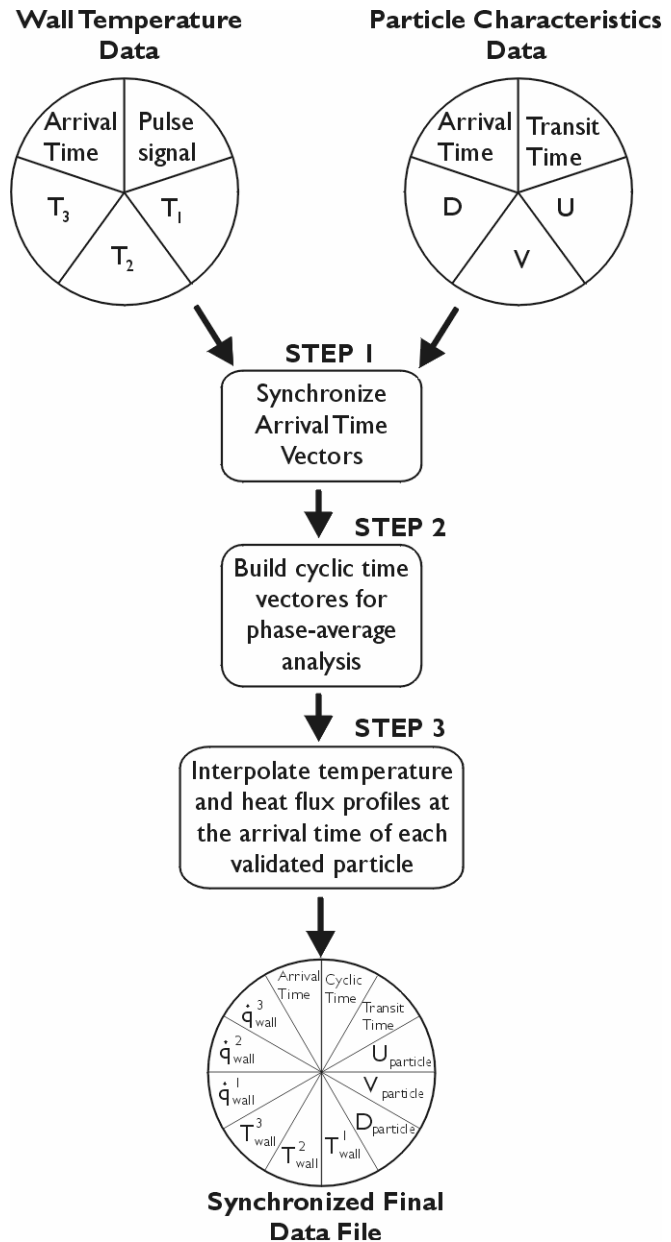


Fig. 5 Diagram of the procedure of generating a data file of synchronized data

Once the three steps are completed, the final output data file contains the following information for each validated droplet: arrival time; cyclic time; transit time; axial and radial velocities; size; wall temperature measured by the three thermocouples ($T_w^{1 \text{ and } 3}$ – lateral positions, T_w^2 – central position, align with the

injector central axis); and the wall heat flux removed by the spray at each thermocouple position ($q_w^{1,2 \text{ and } 3}$). Examples of T_w^2 , axial velocity and V-U correlation from a synchronized output file are shown in Fig. 7. It is noteworthy to observe that the axial velocity profile and the V-U correlation show a considerable number of droplets with a negative axial velocity generated by secondary atomization at the heated wall. In this case, since measurements were made 5 mm above the surface, it is not possible to draw any conclusions about the spray/wall interaction phenomenon.

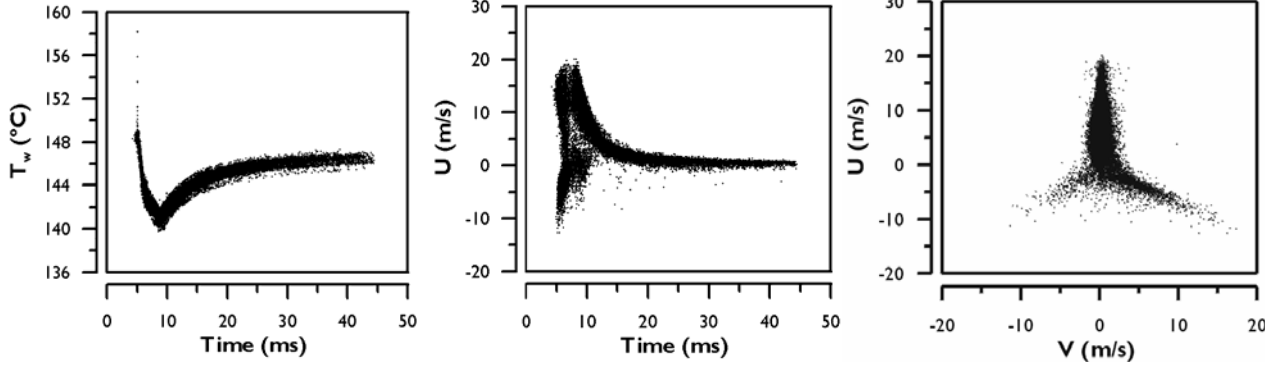


Fig. 7 Examples of temperature and axial velocity temporal profiles and a V-U plot for a synchronized output data file.

2.4 Phase-Average Analysis

Phase average analysis was performed within time windows of 0.5 ms and with a minimum of 200 samples resulting in an inaccuracy better than 9.4% in mean drop size (Tate, 1982) and better than 10% in PDA flux measurements (Saffman, 1987). Table 2 describes the quantities considered in the analysis.

Table 2 – Quantities used in phase-average analysis

Quantity	Expression
$T_w, q_w, \langle U \rangle$	Ensemble average: $\langle \beta \rangle(t) = \frac{1}{N(t)} \sum_{i=1}^{N(t)} \beta_i$
D_{10}	$D_{ij}(t) = \frac{\sum_{i=1}^{N(t)} D^i}{\sum_{i=1}^{N(t)} D^i}$
PDA flux quantities	$\dot{B} = \frac{1}{\Delta t} \sum_{i=1}^{N_w} \frac{\eta_{vi} \cdot \beta_i \cdot \cos(\gamma_i)}{A_\gamma(D_k, \gamma_k)}$

In table 2, β is an arbitrary quantity, which in the case of the PDA flux calculation may be the number, mass, momentum, kinetic energy or surface energy flux at time t . $N(t)$ is the sample size at time t , D_{10} is the arithmetic mean diameter, η_{vi} is a correction factor considering multiple scattering due to the presence of more than one droplet inside the detection volume, $A_\gamma(D_k, \gamma_k)$ is the cross section area of the measurement volume, which is size and direction dependent (for more details on η_{vi} and $A_\gamma(D_k, \gamma_k)$, see Roisman and Tropea, 2001), and, finally, γ is the particle direction defined as $\gamma = \text{atan}(V/U)$. The post-process algorithm calculates other flow characteristics, but only those described in table 2 where considered in the present analysis.

3. RESULTS AND DISCUSSION

A parametric study is reported here on the influence of wall temperature (T_{w0}), injection pressure (p_{inj}) and pulse duration (Δt_{inj}) on the wall heat flux (q_w). The experiments were performed for several boundary conditions as listed in table 3 and the analysis of the results consider the effect of wall temperature on the spray prior to impact. The fuel temperature was measured during each experiment and found to be constant and equal to 31°C.

Table 3 – Boundary conditions of test cases

	p_{inj} (bar)	Δt_{inj} (ms)	T_{w0} (°C)
Case 1	3	5	50
Case 2	3	5	75
Case 3	3	5	100
Case 4	3	5	125
Case 5	3	5	150
Case 6	3	5	250
Case 7	3	10	150
Case 8	4.5	5	50
Case 9	4.5	5	150
Case 10	4.5	10	150

3.1 Spray Dynamic Behaviour

As reported in Panão and Moreira (2004), the transient behaviour of the spray may be divided in three periods, as illustrated in Fig. 8 in terms of the mean axial velocity and size of the impacting droplets for cases 9 and 10. The first period, or the *leading front of the spray*, is characterized by a sudden expansion of the liquid after pintle opening, resulting in a local minimum of the mean axial velocity at the end of the period and a large negative gradient of the mean drop size. The second period, *the steady spray*, starts when the mean drop size attains a plateau value. It lasts up to the end of injection (EOI) and the mean droplet axial velocity increases up to a steady value. During the third and final period, which corresponds to the *spray tail* and starts after the EOI, only small droplets remain suspended in the air with a mean axial velocity decreasing asymptotically down to 0 m/s.

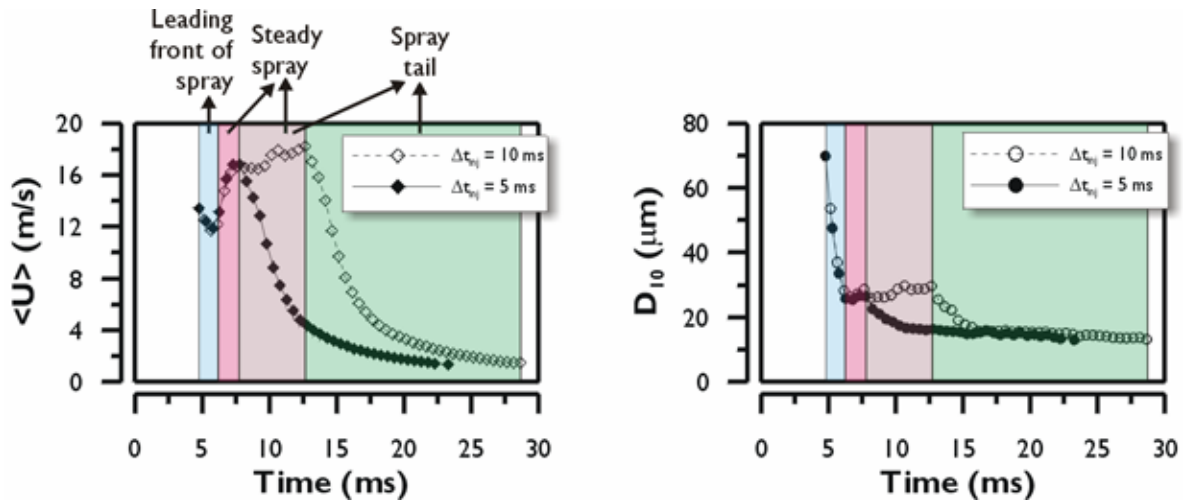


Fig. 8 Transient behaviour of the spray in terms of the mean axial velocity ($\langle U \rangle$) and size (D_{10}) of droplets in cases 9 and 10.

3.2 Effect of Wall Temperature on the Heat Flux removed by Spray Cooling

The heat transfer between an impinging spray and the target surface is governed by flow and fluid thermal properties, as well as by surface roughness and temperature. However, in a liquid/solid system, surface temperature is generally quoted as the single most important parameter determining different heat transfer regimes, which are usually described in a boiling curve. Such curves are not available for the liquid fluid used in the present experiments and only Tamura and Tanasawa (1959) reported measurements but of the lifetime of a motor gasoline droplet deposited onto a heated surface, as shown in Figure 9 for a droplet with 1.74 mm in diameter. Assuming that heat transfer with the surrounding air is negligible, which may not be far from true for a droplet of this size, the evaporation rate and, hence droplet lifetime, may be viewed as inversely proportional to the heat transfer rate between the liquid and the surface. The lifetime curve shows a local minimum and a local maximum corresponding to the Critical Heat Flux (CHF), or Nukiyama temperature, and to the Leidenfrost temperature, respectively. Given that the gasoline liquid saturation temperature (T_{sat}) is 60°C, four regimes may be considered according to the analysis of Naber and Farrel (1993) as depicted in Figure 9:

1. Film Evaporation: $T_w \leq T_{sat}$;
2. Vaporization/Boiling: $T_{sat} \leq T_w \leq T_{Nukiyama}$;
3. Transition: $T_{Nukiyama} \leq T_w \leq T_{Leidenfrst}$;
4. Spheroidal Evaporation/ Leidenfrost: $T_w \geq T_{Leidenfrost}$.

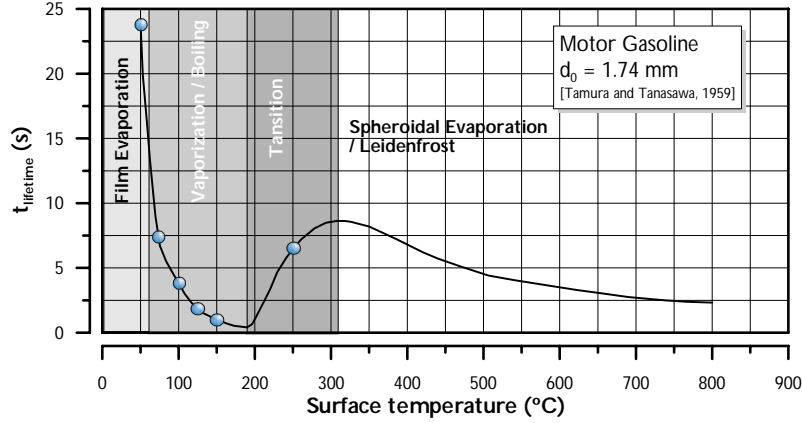


Fig. 9 Lifetime of a 1.74 mm droplet of motor gasoline deposited onto a heated surface as reported by Tamura and Tanasawa (1959).

In the film evaporation and boiling regimes, there is a liquid film in contact with the surface. This is, therefore, considered as the *wetting regime*. In the *transition* regime, the liquid is in contact with the surface only intermittently, due to separations from the surface caused by vapour expelled from the liquid. Above the Leidenfrost temperature, a thin vapour layer is formed between the liquid and the surface, resulting in a *non-wetting regime*. The symbols superimposed to the line in Figure 9 identify the experimental conditions reported in the paper. These were chosen in accordance with the range of maximum temperatures observed in spark-ignited engines with port fuel injection, where inlet valves may be at up to 160°C (Arcoumanis *et al.* 1997) and the piston head at up to 300°C (Li, 1982). Therefore, for $T_w = 50^\circ\text{C}$, 75°C and 100°C (cases 1, 2 and 3 of Table 3) a liquid film is expected to form at the surface, although very thin in the latter case. For larger values of surface temperature, evaporation upon spray impact is too intense and avoids film formation.

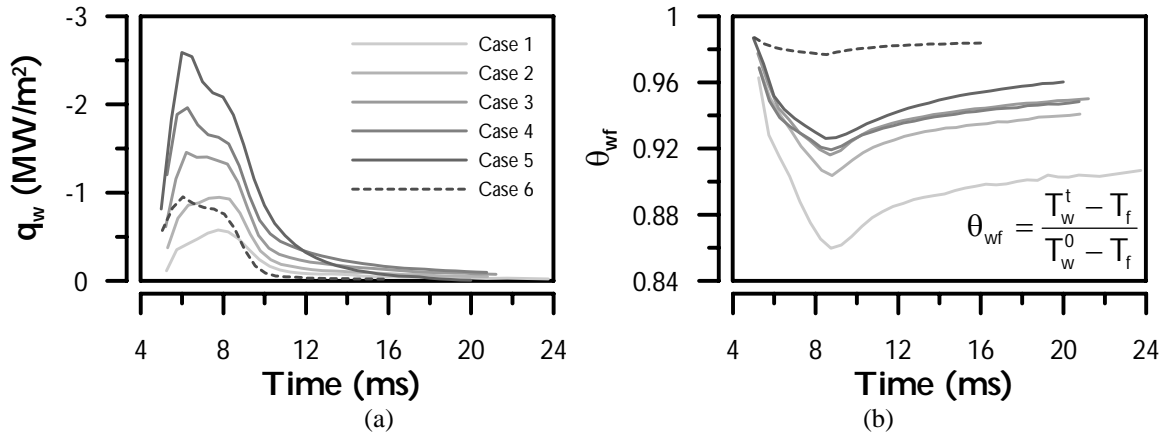


Fig. 10 Temporal variation of (a) wall heat flux; (b) normalized wall temperature for cases 1-6.

Fig. 10 shows the time variation of the wall heat flux and of the normalized wall temperature (θ_{wf}) measured for surface temperatures from 50°C to 250°C and with $p_{inj} = 3$ bar (cases 1 – 6 in Table 3). In general, the effect of surface temperature in the time variation of the heat flux is consistent with the lifetime curve depicted in Fig. 9 in that the total heat flux, identify by the area behind the curve, increases as the surface temperature approaches the CHF point and decreases once this point is surpassed ($T_w = 250^\circ\text{C}$).

The results in Figure 10-(a) show that the heat flux increases continuously after spray impact up to a maximum value and decreases thereafter. But two different behaviours are observed: in the former the heat flux decreases at a continuously decreasing rate after having attained the maximum value, (for example cases 1 and 2); in the second the

heat flux curve has an inflection after the maximum (for example cases 4 and 5). Each behaviour is associated with different impact conditions, as inferred from direct visualization of the flow not reported here. For small temperatures of the target surface, a liquid film is seen to be present at the target, prior to each injection. The evaporation rate of the film increases with surface temperature and is no longer present for temperatures above 100°C (case 3). When the wall temperature is sufficiently high to evaporate the liquid film almost completely between consecutive injection cycles, a peak emerges in the heat flux profile associated with the leading front of the spray. This is accordance with the results reported for $T_w = 75^\circ\text{C}$ and $T_w = 250^\circ\text{C}$ (cases 2 and 6) which, although have similar values of the heat flux, behave differently according to the different evaporation degrees of the liquid film, considerably stronger in the latter case. However, the normalized temperature profiles depicted in Fig. 10-(b) show that the greater relative decrease in the wall temperature occurs for $T_w = 50^\circ\text{C}$ (case 1). When the heat transfer coefficient is computed as $h_w(t) = q_w(t) / (T_f - T_w(t))$, the maximum value is obtained for this temperature and decreases as the temperature increases, although for $T_w = 125^\circ\text{C}$ and $T_w = 150^\circ\text{C}$ (cases 4 and 5) the profiles of h_w are very similar. These results apparently indicate that spray cooling with a pulsed spray is more effective if the impact is made against a liquid film than a dry hotter surface.

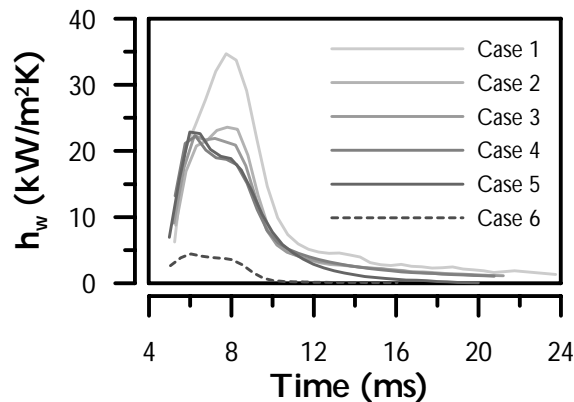


Fig. 11 Temporal variation of the heat transfer coefficient during injection for cases 1 to 6.

3.3 Effect of Injection Pressure and Pulse Duration on Wall Heat Flux

Pressure and duration of injection may influence the transient behaviour of the heat flux, since they alter spray characteristics, drop-air interaction prior to impact and also spray transient behaviour. Figure 12 shows the result of increasing the pressure of injection from $p_{inj} = 3 \text{ bar}$ to $p_{inj} = 4.5 \text{ bar}$ on the time varying convection coefficient, average droplet velocity and arithmetic mean diameter. It is worth-mentioning at this point that values of droplet characteristics reported here can not be correlated with the convection coefficient because PDA measurements were obtained at a distance of 5 mm from the wall. Most of spray-wall interaction occurs at a distance much closer to the surface (e. g., Panão and Moreira, 2004b). This is because the width of the target surface required to accommodate the cross flow does not allow to place the measurement volume of the PDA closer to the surface without blocking the laser beams in the perpendicular plane.

The results depicted in Fig. 12 show an overall decrease of the heat transfer coefficient when pressure increases, although larger for $T_w = 50^\circ\text{C}$ than for $T_w = 150^\circ\text{C}$. A smaller injection pressure is shown to be associated with bigger and slower drops impinging on the wall, which have shorter heat-up and evaporation times. This may therefore be the cause for the observed increase of the convection coefficient. As pressure increases, the mean size of droplets decreases. The resulting greater interaction with the surrounding air and better dispersion is expected to enhance evaporation prior to impact which may be associated with the observed decrease of the heat transfer coefficient. Similar results were also reported by Meingast *et al.* (2000, 2001), although their experiments were performed for diesel engine conditions.

The direct effect of increasing the duration of injection on the dynamic characteristics of the spray is to enlarge the steady period of the spray defined in Figure 8. The consequence is shown in Figure 13 to be an increase of the overall heat flux. However, the heat transfer coefficient, and consequently the heat flux, does not attain a steady period, but instead decreases along the injection, for the lower pressure, while for $p_{inj} = 4.5 \text{ bar}$ the heat flux attains a steady period. Moreover, while the axial velocity profile does not appear to have much influence on the temporal behaviour of the convection coefficient, a similar behaviour is observed between the mean drop size and the heat transfer coefficient, where a larger size is associated with a larger heat transfer coefficient. This result suggests that control of the mean drop size during injection may allow controlling the heat flux behaviour.

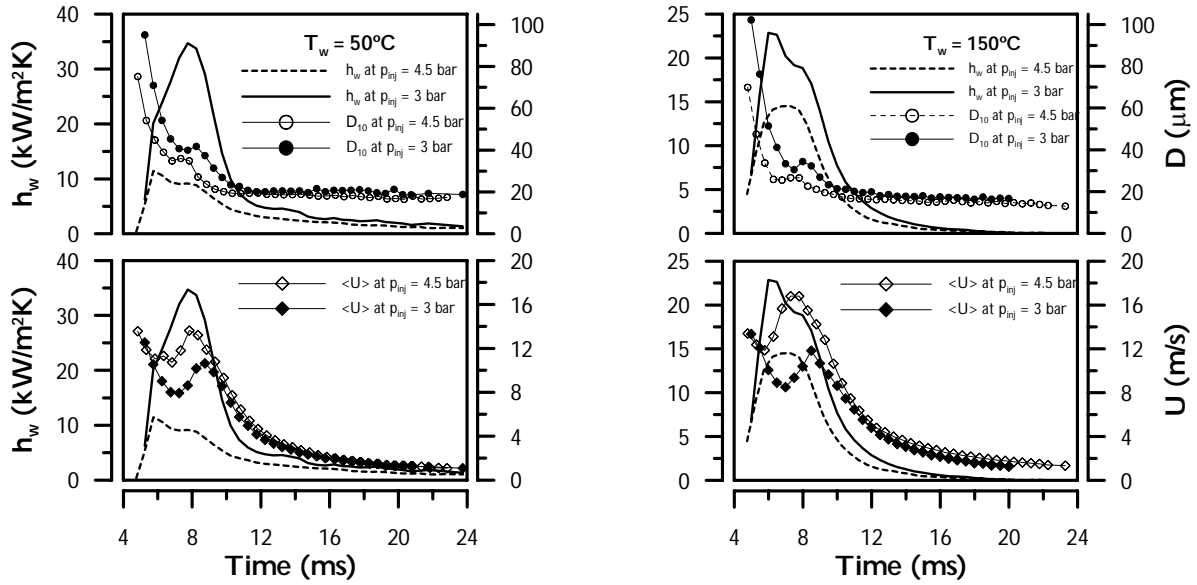


Fig. 12 Effect of injection pressure on the heat transfer coefficient, mean drop size and axial velocity for a duration of injection of 5 ms

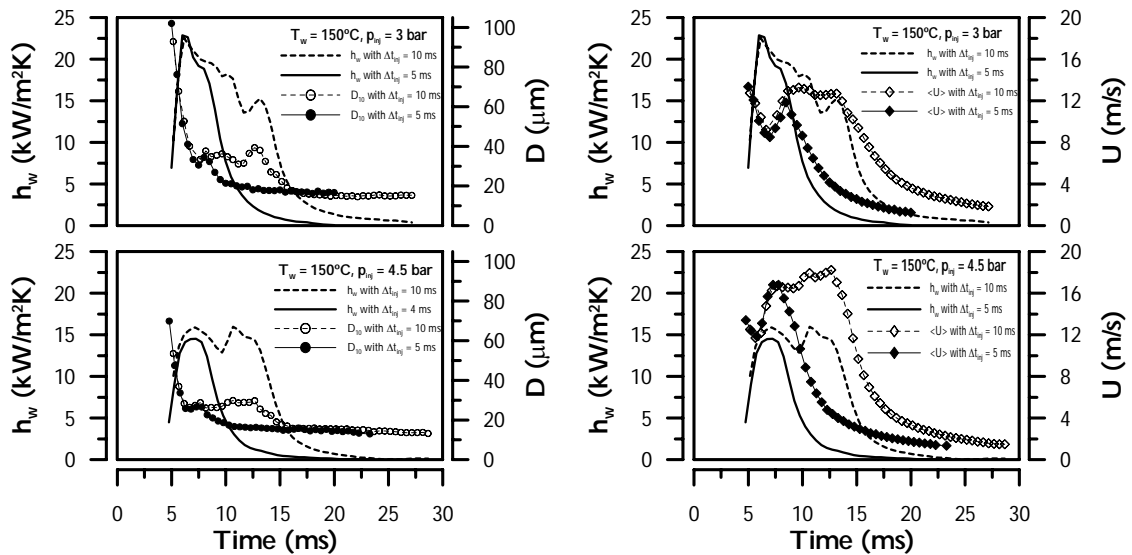


Fig. 13 Effect of duration of injection on the heat transfer coefficient, mean drop size and axial velocity.

3.4 Effect of the Wall Temperature on the Spray Prior to Impact

It has been reported that the thermal interaction of the spray with the surface may be altered by the buoyant jet arising from the heated. Analysis of these effects for the present experimental conditions are inferred from Figure 14, where measurements of mean drop size and velocity made during injection for several surface temperature are normalized by the corresponding values measured for $T_w = 50^\circ\text{C}$. For easy of analysis, the plot also includes the three periods of the spray dynamics defined in section 4.1: 1 – the leading front of the spray up to 6.28 ms; 2 – the steady spray between 6.28 and 7.78 ms; and 3 – the spray tail thereafter.

In general, the results show that mean drop size decreases as the wall temperature increases. This may be attributed, either to partial vaporization of the down moving droplets by the heated rising plume, or to secondary atomization induced by thermal effects as also suggested by Özdemir and Whitelaw (1993) based on measurements made at 5.5 mm from the surface. This is corroborated by the observed increase of the number flux of droplets in the axial direction as

represented in Figure 15. The plot shows that the number flux of droplets increases with wall temperature, thus suggesting that reduction of surface tension of the inflowing droplets by the thermal plume emerging from the heated surface may promote break-up.

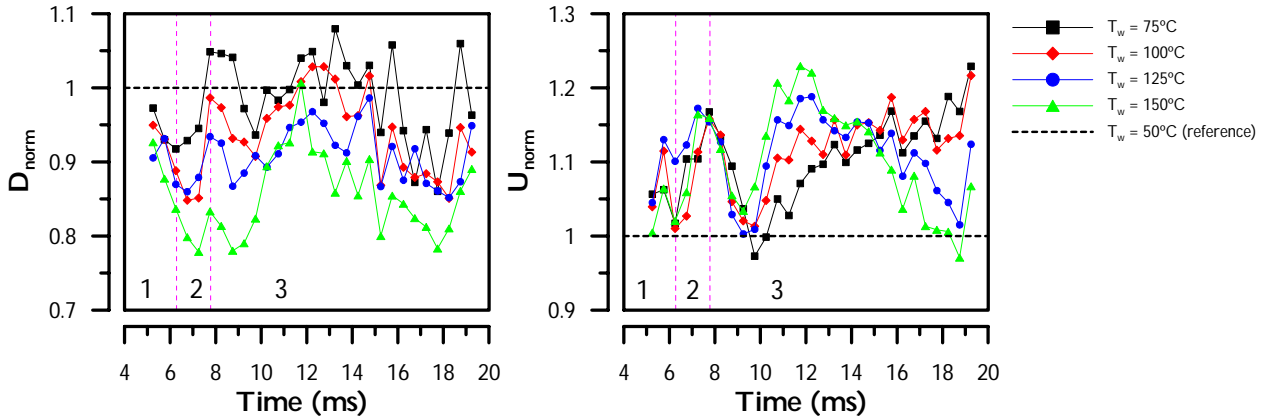


Fig. 14 Time variation of dimensionless mean drop size and velocity when surface temperature ranges from $T_w = 75^\circ\text{C}$ to $T_w = 250^\circ$ for $p_{in} = 3$ bar and $\Delta t_{inj} = 5$ ms. (Normalization is made with corresponding values at $T_w = 50^\circ\text{C}$)

In what concerns the time variation of mean droplet velocity in Figure 14, values are up to 15% larger than at the reference state until 10 ms ASOI. However, larger differences are seen at the spray tail, and are associated with small secondary droplets which are entrapped by the time growing toroidal vortex and remain suspended in the air between consecutive injections, as reported in Panão and Moreira (2004). Closer analysis shows that thermal-induced variations of the mean velocity within the spray tail behave differently up about 15 ms and later. Within the first period, mean droplet velocity increases with surface temperature, suggesting that evaporation of droplets with lower velocities dominates over drag effects induced by the thermal plume. Reduction of droplet velocity due to saturated buoyant jet as observed by González and Black (1997) only occurs later within the spray tail, when droplets are more prone to drag.

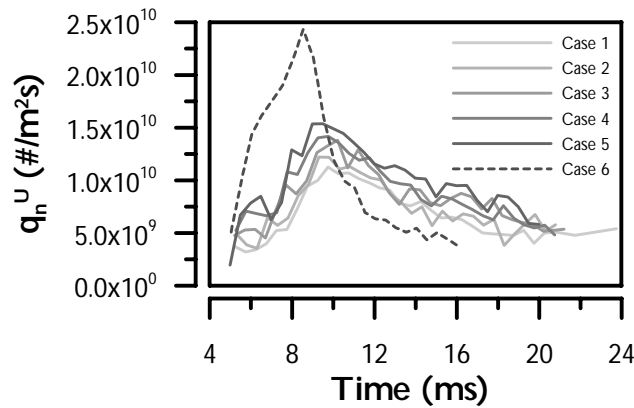


Fig. 15 Time variation of the axial number flux of droplets prior to impact when surface temperature ranges from $T_w = 75^\circ\text{C}$ to $T_w = 250^\circ$ for $p_{in} = 3$ bar and $\Delta t_{inj} = 5$ ms

4. SUMMARY AND CONCLUDING REMARKS

In this paper a methodology is described to provide simultaneous data on transient droplets characteristics and wall temperature at spray impingement. It consists on combining temperature data acquired by a dedicated DAQ with droplet data acquired by a PDA system. Post-process software synchronizes the arrival time vector of both data files using the pulse sent to the liquid injector as the reference time. Once temperature data and droplets characteristics are synchronized, a final data file is generated by considering temperature equivalent to a continuous phase in a multiphase flow. Thus, for each particle crossing the detection volume a wall temperature measurement is obtained by interpolation at the corresponding time instant.

The method is tested in a flow consisting of an intermittent gasoline spray that forms a toroidal wall-jet vortex upon impact. The vortex was previously reported to play an important role on the fluid-dynamic interaction since it entrains smaller and, thus, more responsive droplets produced by secondary atomization mechanisms such as splash, rebound and film stripping. The objective here is to perform a parametric analysis on the influence of the wall temperature, injection pressure and duration on the heat removed from the surface, on the heat transfer coefficient and on the dynamic characteristics of droplets during injection. Measurements are performed at the geometrical axis of the injector at 5 mm above the wall and allow evaluating the influence of the heated surface on the spray characteristics prior to impact.

The results show that the heat flux increases with increasing the temperature of the target, although the convection coefficient decreases. Two regimes of thermal interaction between the spray and the target may occur during the period of injection, depending on the temperature of the target. Only for large initial values of the target temperature, the liquid film remaining on the surface between injections evaporates completely and interaction occurs with an initially dry surface. Results suggest that heat transfer rates during the initial phase are enhanced when the surface is wetted.

Experiments further show that the overall heat transfer coefficient increases when the pressure of injection decreases and/or the duration of injection increases, which is attribute to different dynamic behaviours of thermal spray-wall interaction.

Surface heating is observed to alter the behaviour of the spray prior to impact in two ways: during injection it enhances evaporation, later in the spray tail it induces secondary break-up of droplets and only at a last stage, when very small droplets remain suspended within the air, drag forces induced by the rising plume dominate.

Future work will include the application of the acquisition system and methodology to study spray/wall interaction aiming at correlating the incident spray with the wall heat flux and the mechanisms of secondary atomization.

REFERENCES

Arcoumanis, C. and Chang, J – C. (1994) “Flow and Heat Transfer Characteristics of Impinging Transient Diesel Sprays”, SAE Technical paper 940678

Arcoumanis, C. and Chang, J.-C. (1993) “Heat transfer between a heated plate and an impinging transient diesel spray”, *Experiments in Fluids*, 16, pp. 105-119.

Arcoumanis, C., Whitelaw, D.S. and Whitelaw, J.H. (1997), “Gasoline injection against surfaces and films”, *Atomization and Sprays*, 7, pp. 437-456.

Cowart, J. and Cheng, W. (1999), “Intake Valve Thermal Behavior During Steady-State and Transient Engine Operation”, SAE Technical Paper, 1999-01-3643.

Cutter, P. (1996) “Diesel Spray Characteristics, Spray/Wall Interaction and Heat Transfer”, PhD Thesis, Imperial College of Science, Technology and Medicine, University of London.

González, J.E. and Black, W.Z. (1997) “Study of Droplet Sprays Prior to Impact on a Heated Horizontal Surface”, *ASME Journal of Heat Transfer*, 119, pp. 279 – 287.

Jia, W. and Qiu, H.-H. (2003), “Experimental investigation of droplet dynamics and heat transfer in spray cooling”, *Experimental Thermal and Fluid Science*, 27, pp. 829-838.

- Li, C.-H. (1982), "Piston thermal deformation and friction considerations", SAE Technical Paper 820086.
- Meingast, U., Reichelt, L. and Renz, U. (2001), "Measuring transient wall heat flux under diesel engine conditions", 5th Int. Symp. Diag. and Modeling of Comb. In IC Eng., COMODIA 2001, Nagoya, pp. 140-146.
- Meingast, U., Staudt, M., Reichelt, L., Renz, U. and Sommerhoff, F.-A. (2000), "Analysis of spray/wall interaction under diesel engine conditions", SAE Technical Paper 2000-01-0272.
- Naber, J.D. and Farrel, P.V. (1993), "Hydrodynamics of droplet impingement on a heated surface", SAE Technical Papers 930919.
- Özdemir, I.B. and Whitelaw, J.H. (1993) "Impingement of an unsteady two-phase jet on unheated and heated flat plates", J. Fluid Mechanics, 252, pp. 499-523.
- Panão, M.R. and Moreira, A.L.N. (2002a) Visualization and Analysis of Spray Impingement under Cross-Flow Conditions, SAE Technical Paper 2002-01-2664.
- Panão, M.R. and Moreira, A.L.N. (2002b) Spray Impingement on a Flat Plate under Cross-flow Conditions, Proceedings of the 18th A. Conf. Liquid Atom. Spray Systems, Zaragoza.
- Panão, M.R.O. and Moreira, A.L.N. (2004), "Experimental study of the flow regimes resulting from the impact of an intermittent gasoline spray", to appear in Experiments in Fluids.
- Reichelt, L., Meingast, U. and Renz, U. (2002) "Calculating transient wall heat flux from measurements of surface temperature", Int. Journal of Heat and Mass Transfer, 45, pp. 579-584.
- Roisman, I.V. and Tropea, C. (2001), "Flux measurements in sprays using phase Doppler techniques", Atomization and Sprays, 11, pp. 667-700.
- Saffman, M (1987), "Automatic calibration of LDA measurement volume size", Applied Optics, 26, pp. 2592-2597.
- Shayler, P. J., Colechin, M. J. F. and Scarisbrick, A. (1996) "Fuel Film Evaporation and Heat Transfer in the Intake Port of an S. I. Engine", SAE Technical paper 961120.
- Tamura, Z. and Tanasawa, Y. (1959), "Evaporating and combustion of a drop contacting with a hot surface", 7th Symp. (Int.) on Combustion, pp. 509-522.
- Tate, R.W. (1982), "Some problems associated with the accurate representation of droplet size distributions", Proceedings of the 2nd Int. Conf. Liquid Atom. And Spray Systems, Madison.
- Yoshida, K., Abe, Y., Oka, T., Mori, Y.H., and Nagashima, A. (2001), "Spray cooling under reduced gravity conditions", ASME Journal of Heat Transfer, 123, pp. 309-318.